X-ray spectra of model binary alloys $A_{1-x}B_x$

Marshall A. Bowen
Department of Physics, Western Illinois University, Macomb, Illinois 61455

John D. Dow
Department of Physics, University of Notre Dame, Notre Dame, Indiana 46556

(Received 14 January 1985)

The x-ray photoemission, absorption, and emission spectra of a one-dimensional tight-binding model for a binary metallic alloy $A_{1-x}B_x$ are evaluated in a change of mean-field model. The combined effects of disorder and multielectron excitations are included. The extent of the asymmetric tails of the x-ray photoemission lines depend on the local character of the Fermi-energy states in the vicinity of the core hole; this effect could explain the long-standing mystery of why Na 1s lines in Na_xWO_3 are symmetric. Features in the absorption and emission spectra reminiscent of the anomalous ramplike thresholds observed for absorption by rare-gas atoms in alkali-metal hosts are also found.

I. INTRODUCTION

As a first step toward understanding the x-ray absorption, emission, and photoemission spectra of binary alloys, we present here the results of model calculations for a one-dimensional, substitutional, crystalline, binary alloy $A_{1-x}B_x$. The model treats a single orbital and a single electron per site in a nearest-neighbor tight-binding approximation. Many-electron effects due to the final-state interactions of the electrons with the core hole are treated in a change-of-mean-field approximation.[1] Hence, the model exhibits features associated with both the "x-ray edge anomalies"[2–4] and binary-alloy disorder.[5] To our knowledge, this is the first study of the combined effects on x-ray spectra of disorder in a binary-alloy and many-electron recoil.

II. MODEL

The one-electron Hamiltonian governing the behavior of the alloy is

$$h=\sum_{n=1}^{M}\epsilon(n)\,|\,n)(n\,|+\beta\,|\,n)(n+1\,|+\beta\,|\,n+1)(n\,|\ . \tag{1}$$

Here we have M sites, $|\,n)$ refers to the one-electron orbital centered at the nth site, β is the nearest-neighbor transfer matrix element, and $\epsilon(n)$ is a random variable which takes on the values ϵ_A (with probability $1-x$) and ϵ_B (with probability x).

In the case of x-ray photoemission the band has N electrons in both the initial and final states, but the initial-state N-electron Hamiltonian

$$H_I=\sum_{i=1}^{N}h_i \tag{2}$$

changes suddenly as a result of the removal of the core electron to the final-state Hamiltonian

$$H_F=\sum_{i=1}^{N}h_i'\ , \tag{3}$$

where we have

$$h'=h+V_0\,|\,\mathbf{R})(\mathbf{R}\,|\ , \tag{4}$$

with $|\,\mathbf{R})$ referring to the orbital centered on the core-hole site; V_0 is the electron-hole interaction strength (and a negative number). The initial many-electron state of the electron gas $|\,I\rangle$, in this model, is a Slater determinant of the lowest-energy single-particle eigenstates $|\,\phi)$ of h; the final states $|\,F\nu\rangle$ are all the various determinants of the eigenstates $|\,\psi)$ of h'.

The x-ray photoemission spectrum is

$$I(E)=\sum_{\nu}|\,\langle I\,|\,F\nu\rangle\,|^2\delta(E+E_{F\nu}-E_I-\hbar\omega-\epsilon_{\rm core})\ , \tag{5}$$

where the summation is over all possible final-state configurations. The photoemission recoil energy is

$$E_{F\nu}-E_I\equiv\sum_{i}^{N}\epsilon_i'-\sum_{i}^{N}\epsilon_i\ , \tag{6}$$

where the sums are over all occupied one-electron states in the electronic configurations $|\,F\nu\rangle$ and $|\,I\rangle$, respectively. The photoemission line shape has contributions from both spin-up and spin-down channels. It can be shown, however, that one can evaluate the line shapes for each of these channels independently and that the two-channel line shape is a convolution of the single-channel shapes.[1] Hence, for simplicity of presentation we consider here only the spin-up channel, and we have $M=2N$.

X-ray emission of a photon of energy E can be treated in a manner completely analogous to photoemission, and has a line shape

$$\kappa(E)=\sum_{\nu} |\langle F\nu | M | I\rangle|^2 \delta(E-E_I+E_{F\nu}) , \tag{7}$$

where the final states $|F\nu\rangle$ are Stater determinants of N $|\phi)$'s and one core orbital and the initial state is a determinant of $N+1$ $|\psi)$'s. A similar expression holds for x-ray absorption.[6] We assume that the core hole has a negligible radius, in which case the dipole matrix element M can be simplified, and we have

$$\langle F\nu | M | I\rangle = M_0 \begin{vmatrix} \psi_1(\mathbf{R}) & \psi_2(\mathbf{R}) & \cdots & \psi_{N+1}(\mathbf{R}) \\ (\phi_{\nu,1}|\psi_1) & & & \\ (\phi_{\nu,2}|\psi_1) & & & \\ \cdots & & & \\ (\phi_{\nu,N}|\psi_1) & \cdots & & (\phi_{\nu,N}|\psi_{N+1}) \end{vmatrix} . \tag{8}$$

Here $\psi(\mathbf{R})$ is proportional to the overlap of $|\psi)$ with the core hole at site $\mathbf{R}$, M_0 is a constant, $(\phi|\psi)$ is a scalar product, and we have assumed that the core hole has a negligible radius.[6]

The line shapes $I(E)$ and $\chi(E)\equiv\kappa(E)/M_0^2$ are calculated as follows: The eigenstates $|\phi)$ and $|\psi)$ and the corresponding eigenvalues are evaluated for a one-dimensional lattice with $M=40$ sites occupied by a specific configuration of atoms A and B, as determined by a random-number generator. The core hole is confined to one of the ten innermost sites. The matrix elements between determinants, such as $\langle I|F\nu\rangle$, are evaluated for many electronic configurations ν and the spectra are calculated. The calculation of a given spectrum is terminated (i.e., no more configurations ν are included) when the sum rules for x-ray photoemission spectra[1] (XPS)

$$\int_{-\infty}^{\infty} I(E)dE=1 \tag{9}$$

and for emission[6]

$$\int_{-\infty}^{\infty} \chi(E)dE=\sum_i |\psi_i(\mathbf{R})|^2 \tag{10}$$

are adequately exhausted (the sum is over occupied initial-state orbitals ψ_i). The calculations are repeated for (typically $\simeq$100) different atomic configurations and (typically $\simeq$10 per atomic configuration) different core-hole sites, Gaussian broadened[7] and ensemble averaged. The ensemble-averaged spectra are displayed in Figs. 1 to 6 for $\beta=-\frac{1}{2}$, $V_0=-2|\beta|$, $\epsilon_B=2|\beta|$, and $\epsilon_A=-2|\beta|$ for $x=0.2$, 0.4, 0.6, and 0.8.

III. RESULTS

The results can best be understood in terms of the broadened[7] densities of states displayed in Fig. 7. In all cases the Fermi surface lies within a band and the system is metallic.

A. X-ray photoemission spectra

For a core hole created at an A site (Fig. 1), the x-ray photoemission spectra exhibit long tails associated with low-energy excitation of Fermi-surface electrons for $x=0.2$ and 0.4, but not for $x=0.8$ or 0.6. The reason for this is that the one-electron states near the Fermi surface are A-like for $x=0.2$ and 0.4, but are B-like for $x=0.8$ or 0.6 (see Fig. 7). Only the A-like states are efficiently excited as the shock wave due to the A-site core-hole creation propagates outward. The B-like electron states at the Fermi energy for $x=0.6$ and 0.8 do not thoroughly overlap with and couple to the A-site core hole, and are not so easily excited as a result of the core-hole creation. Hence, the A-site XPS lines for $x=0.6$ and 0.8 do not have long tails for negative $E-\hbar\omega-\epsilon_{\text{core}}$, but the lines for $x=0.2$ and 0.4 do. (Similarly, creation of a B-site core hole produces a long XPS tail for $x>0.5$ but not for $x<0.5$, as shown in Fig. 2.) Thus we have a clear dependence of the shape of the XPS line on the char-

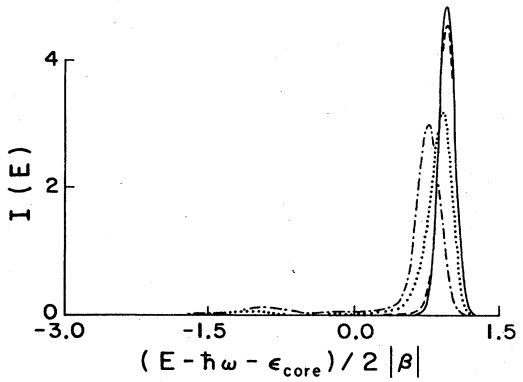

FIG. 1. Predicted x-ray photoemission spectra for core excitation of the A site in $A_{1-x}B_x$ as a function of the emitted electron's energy E, for $x=0.2$ (dash-dotted line), $x=0.4$ (dotted line), $x=0.6$ (dashed line), and $x=0.8$ (solid line).

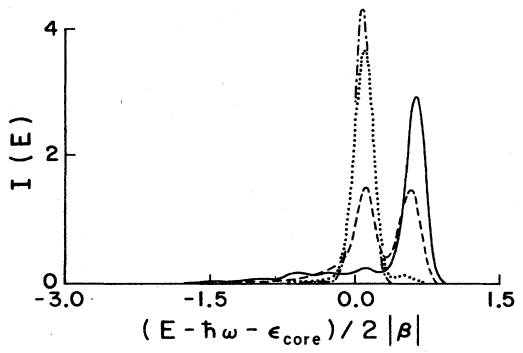

FIG. 2. Predicted B-site x-ray photoemission spectra, as in Fig. 1.

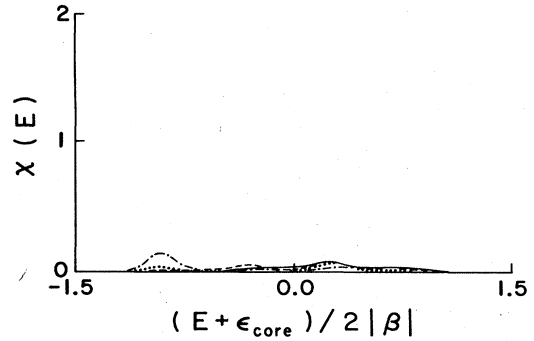

FIG. 3. Predicted x-ray absorption spectra $\chi(E)$ for excitation of a core level at the A site, with notation as in Fig. 1.

acter of the Fermi-energy electrons at the site of the core hole.

The asymptotic theory of Doniach and Sunjic[4] for excitation of a free-electron gas is valid for electron energies E near the photoemission threshold energy E_T and gives an XPS line shape

$$I(E) \propto (E_T - E)^{-1+\Delta} \Theta(E_T - E) , \tag{11}$$

where Θ is the unit step function and the exponent Δ is expressible in terms of δ_l, the change of Fermi-energy phase shifts of an electron as a result of the potential of the core hole:

$$\Delta = \sum_{l=0}^{\infty} 2(2l+1)(\delta_l/\pi)^2 . \tag{12}$$

This asymptotic line shape does not depend on the character or density of states near the Fermi energy, except through the phase shifts δ_l. Nevertheless, our calculations, which solve a Doniach-Sunjic type of model for all energies (not just for $E \to E_T$), show that the extent of the XPS tail does indeed depend on the character of the Fermi-energy states.

This behavior may have been observed in sodium-tungsten bronzes: Campagna *et al.*[8] and Chazalviel *el al.*[9] have reported both an asymmetric W XPS line and an excessively symmetric Na 1s XPS line in Na_xWO_3; the latter cannot be explained by the asymptotic theory, [Eq. (11)].[10] It is noteworthy that in the simplest model the Na states do not contribute to the conduction band;[8,9,11]

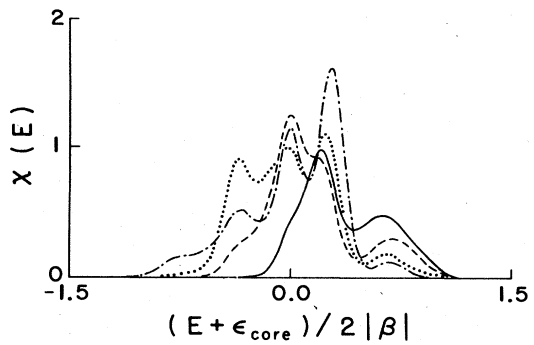

FIG. 4. Predicted B-site x-ray absorption spectra.

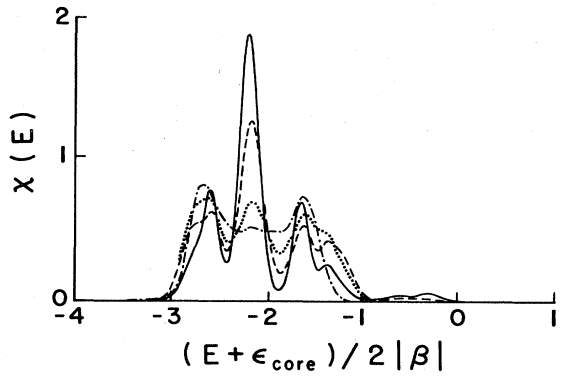

FIG. 5. Predicted A-site x-ray emission spectra.

hence the Na-like character of the Fermi-energy states in Na_xWO_3 should be small—and by analogy with the present results we expect the Na XPS line to be quite symmetric. Hence, the present theory indicates that the large asymmetric tail predicted on the basis of the asymptotic Doniach-Sunjic theory should not necessarily be expected when the amplitude of the Fermi-energy one-electron states at the core-hole site is not large — because the electron-hole pair excitations of those states (which are responsible for the long tail) cannot be efficiently achieved.

A second interesting feature of the A-site XPS spectra is the small bump for $x = 0.2$ and 0.4 near $E - \hbar\omega - \epsilon_{\text{core}} \simeq -2|\beta|$ ($= |V_0|$ here), which we associate with transitions of the electron gas that leave a hole in the bound state below the A band. (This bound state always occurs in one dimension and is caused by the attractive electron-hole interaction; it lies of order $\simeq |V_0|$ below the band bottom.)

The XPS spectra at the B site are especially interesting. The lines for $x = 0.2$ and 0.4 are nearly symmetric because the Fermi-energy states are largely A-like and not efficiently excited by a B-site core hole. They are also almost recoilless (viz., at zero energy) because the B-like states that are perturbed by the core hole are unoccupied and therefore do not contribute to the recoil energy [Eq. (6)]. The $x = 0.4$ spectrum has, in addition to its recoilless peak, a weak high-energy peak associated with recoil: The on-site level at ϵ_B is pulled below the Fermi level by

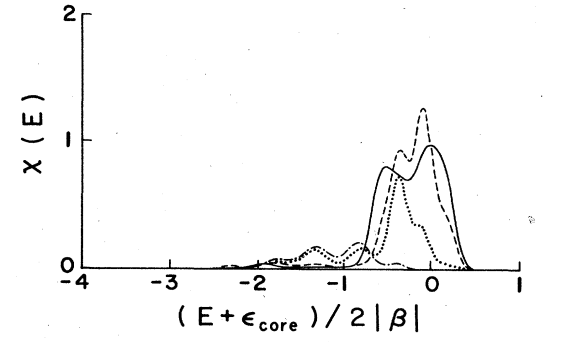

FIG. 6. Predicted B-site x-ray emission spectra.

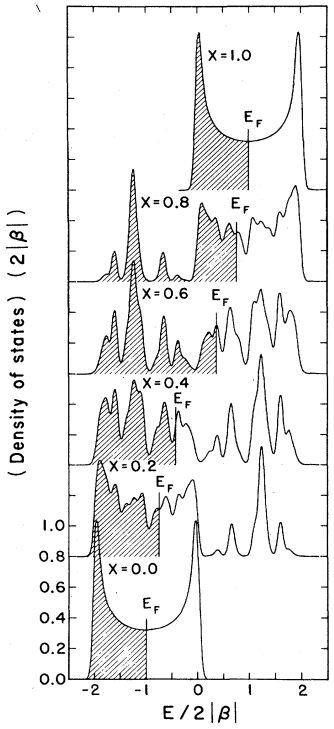

FIG. 7. One-electron density of states (times $2|\beta|$) of $A_{1-x}B_x$ vs E (in units of $2|\beta|$) for $x=0$, 0.2, 0.4, 0.6, 0.8, and 1.0. The Fermi energies are denoted by E_F and occupied one-electron states are shaded. Note that the one-electron states at the Fermi energy are A-like for $x<0.5$ and B-like for $x>0.5$.

the electron-hole interaction, becomes occupied, and contributes to the recoil energy. (This effect was predicted first for d states by Kotani and Toyozawa[12] and then, in a different context, by Mehreteab and Dow.[13]) As the alloy composition x and the Fermi energy increase, local alloy configurations which lead to recoil become more probable and the recoil peak grows as the recoilless peak decreases in amplitude. For $x\simeq 0.8$ the Fermi energy lies within $|V_0|$ of ϵ_B and the recoil peak is dominant. Bumps below the main peak are associated with the alloy disorder.

B. Absorption spectra

The absorption spectra for the core hole on an A site (Fig. 3) are generally weak because of the predominantly B-like character of the unoccupied one-electron states. The strongest spectrum is for $x=0.2$ and corresponds to a case in which there is a reasonable amount of A character to the final state.

For a core hole at a B site the absorption spectra (Fig. 4) are stronger because the B hole couples strongly to the B-like unoccupied electron states. Even for $x=0.2$ there is some B character to the Fermi-energy states, and the absorption edge (at the left of Fig. 4) becomes more abrupt as x and the B character of the Fermi-energy states increases. In general the spectra exhibit low-energy absorption edges and bumps at higher energy that are derived from the hole-perturbed bumps in the densities of states. [The van Hove singularity[14] at the band maximum is weakened both by the matrix element, Eq. (8), and the alloy disorder.]

An especially interesting feature of the calculated B-site spectrum for $x=0.2$ is its low-energy edge — which does not show the expected[2,3] peaked threshold behavior (predicted for free-electron metals):

$$\chi(E)\propto(E-E_T)^{-\alpha_0}\Theta(E-E_T)\ , \tag{13}$$

where E_T is the threshold energy and α_0 is the x-ray edge exponent.[15] Instead, the threshold line shape is very nearly a linear function of energy, $\alpha_0\simeq -1$. Such behavior is what has been observed for rare-gas atoms in alkali-metal hosts by Flynn and co-workers,[16] and has remained a major unexplained anomaly for years.[17] The present work suggests that the "anomaly" may be a consequence of the non-B character of the Fermi-surface states.

C. Emission spectra

The emission spectra for an A-site core hole evolve in an interesting fashion as a function of composition x. For small x, $x=0.2$, the spectrum exhibits a low-energy peak associated with a band-bottom van Hove singularity[14] (see Figs. 5 and 7) that has been partially amputated by disorder; it also has a high-energy edge with a peak reminiscent of an x-ray edge anomaly [Eq. (13), with E and E_T reversed]. For $x=0.4$, 0.6, and 0.8, additional features associated with alloy disorder as manifested in the densities of states (Fig. 7) are reflected in the spectra. In addition, the $x=0.6$ and 0.8 spectra have weak high-energy edges (that are more or less ramplike functions of energy) because the Fermi-energy states are B-like and do not couple effectively to an A hole.

On the B site the spectra are dramatically different, showing bumps associated with the alloy disorder (shifted by the electron-hole interaction), high-energy x-ray edges [Eq. (13)], for $x=0.8$ and $x=0.6$ that weaken as the B character of the Fermi-energy states is lost with decreasing x. For $x=0.8$ there is a high-energy x-ray edge (near $E+\epsilon_{\text{core}}\simeq 0$), the remnants of a van Hove singularity in the density of states (near $E+\epsilon_{\text{core}}\simeq -|\beta|$), and a weak low-energy peak (near $E+\epsilon_{\text{core}}\simeq -4|\beta|$) associated with the density of states: B character is mixed into the A-like states by the alloy. The prominent x-ray edge occurs because the B hole efficiently excites the B-like Fermi-surface particle-hole excitations. For $x=0.6$ to $x=0.2$, qualitatively similar structures appear, most of which are peaks shifted by the electron-hole interaction, but associated with the disorder as reflected also in the densities of states. The strength of the emission weakens as the B character of the Fermi surface is lost (as x decreases). Also, the high-energy x-ray edge weakens and becomes ramplike for $x=0.2$.

D. Summary

In summary the predicted x-ray spectra of one-dimensional $A_{1-x}B_x$ substitutional alloys are rich in

features that are associated with alloy disorder, x-ray edge effects, and van Hove singularities. The effects of alloy disorder found here are probably more pronounced than one would find in three-dimensional alloys, owing to the lack of multiple paths circumventing any highly disordered region. Two particularly interesting features of the calculated spectra appear to hold promise for explaining some old mysteries: (i) The anomalously symmetric XPS lines of sodium-tungsten bronzes appear to be related to the fact that the character of the one-electron states at the Fermi energy is such that these states are not efficiently excited by a Na-site core hole, and (ii) the ramplike linear absorption thresholds of rare-gas atoms in alkali-metal hosts appear to be related to the fact that the Fermi-surface states at the rare-gas site do not have sufficient alkali-metal character. An interesting prediction of the model is that the emission spectrum from rare-gas atoms in alkali-metal hosts should also have ramplike thresholds rather than edge anomalies. It would be gratifying if this prediction were verified experimentally.

ACKNOWLEDGMENT

We are grateful to the U.S. Office of Naval Research for their generous support (under Contract No. N00014-84-K-0352).

[1]J. D. Dow and C. P. Flynn, J. Phys. C **13**, 1341 (1980).
[2]J. Friedel, Comments Solid State Phys. **2**, 21 (1969).
[3]P. Nozières and C. T. de Dominicis, Phys. Rev. **178** 1097 (1969).
[4]S. Doniach and M. Sunjic, J. Phys. C **3**, 285 (1970).
[5]P. Dean, Rev. Mod. Phys. **44**, 127 (1972); Proc. Soc. London, Ser. A **260**, 263 (1961); Proc. Phys. Soc. London **84**, 727 (1964); D. N. Payton and W. M. Visscher, Phys. Rev. **154**, 802 (1967); **156**, 1032 (1967); **175**, 1201 (1968).
[6]C. A. Swarts, J. D. Dow, and C. P. Flynn, Phys. Rev. Lett. **43**, 158 (1979); C. A. Swarts and J. D. Dow (unpublished).
[7]The broadening function is $(2\pi\Gamma^2)^{-1/2}\exp(-x^2/2\Gamma^2)$, with $\Gamma=0.08\,|2\beta|$. For Fig. 7 we used $\Gamma=0.05\,|2\beta|$.
[8]M. Campagna, G. K. Wertheim, H. R. Shanks, F. Zumsteg, and E. Banks, Phys. Rev. Lett. **34**, 738 (1975).
[9]J. N. Chazalviel, M. Campagna, G. K. Wertheim, and H. R. Shanks, Phys. Rev. B **16**, 697 (1977).
[10]J. D. Dow, Philos. Mag. **35**, 837 (1977).
[11]J. B. Goodenough, Prog. Solid State Chem. **5**, 145 (1971); Bull. Soc. Chim. Fr. **1965**, 1200 (1965); L. F. Mattheiss, Phys. Rev. B **6**, 4718 (1972).
[12]A. Kotani and Y. Toyozawa, J. Phys. Soc. Jpn. **37**, 912 (1974).
[13]E. Mehreteab and J. D. Dow, Phys. Rev. B **26**, 2261 (1982); Solid State Commun. **43**, 837 (1982).
[14]L. van Hove, Phys. Rev. **89**, 1189 (1953).
[15]In terms of the Fermi-energy phase shift associated with the electron-hole interaction, we have $\alpha_0=2\delta_0/\pi-\delta_0^2/\pi^2$.
[16]R. A. Tilton, D. J. Phelps, and C. P. Flynn, Phys. Rev. Lett. **32**, 1006 (1974); R. A. Tilton and C. P. Flynn, *ibid.* **34**, 20 (1975); D. J. Phelps, R. Avci, and C. P. Flynn, *ibid.* **34**, 23 (1975).
[17]M. A. Bowen and J. D. Dow, Nuovo Cimento **1D** 587 (1982); M. A. Bowen, D. V. Froelich, and J. D. Dow, Phys. Lett. **102**, 73 (1984).